BIOORGANIC CHEMISTRY 10, 266–276 (1981)

Intramolecular Catalysis of Amide Hydrolysis by Carboxyl and Metal Ion/Proton Agents

I. Intramolecular Reactions of Imidazole or Pyridine Derivatives of Maleamic Acid

JUNGHUN SUH AND DU-JONG BAEK

Department of Chemistry, Seoul National University, Seoul, Korea

Received July 7, 1980

Kinetic studies on the hydrolysis of *N*-(2-imidazolylethyl)maleamic acid, *N*-(2-pyridylethyl)maleamic acid, and *N*-(2-pyridylmethyl)maleamic acid were carried out. In these maleamic acid derivatives, the amide nitrogens together with the heterocyclic nitrogens form bidentate ligands. The compounds were hydrolyzed through nucleophilic catalysis by carboxyl groups. The pH profiles for the hydrolysis at 65°C were descending sigmoids and were unaffected by the ionization of the heterocyclic nitrogens. The absence of rate enhancement due to the added divalent metal ions revealed that chelate formation by the bidentate leaving groups is not efficient. *N*-(2-Pyridylmethyl)maleamic acid underwent a dual intramolecular nucleophilic reaction through participation of both the carboxyl and the pyridyl groups.

INTRODUCTION

Intramolecular catalysis of amide hydrolysis has been extensively studied as a model for proteolytic enzymes (*1–9*). Amide C–N bonds resist cleavage because of resonance stabilization (Eq. [1]).

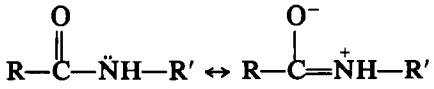

[1]

In addition, the high basicity of the leaving nitrogen anion requires protonation of the nitrogen in the tetrahedral intermediate for facile acyl transfer to an attacking nucleophile. One might expect that coordination of a Lewis acid such as a metal ion or proton on the amide nitrogen would lead to the destruction of the resonance stabilization and the C–N double bond character in the amide bond (Eq. [2]) in addition to enhancing the leaving ability of the amine moiety.

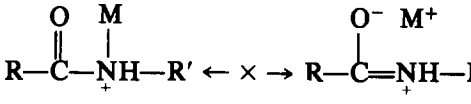

[2]

0045-2068/81/030266-11$02.00/0

Among the studies of catalytic amide hydrolysis, those of intramolecular catalysis by carboxyl groups have been the most extensive (*3–9*). Thus, studies on the hydrolysis of maleamic acid derivatives revealed that the carboxylate group participates as a nucleophile but that maximum rates are obtained when the carboxyl group is not ionized (*3*, *4*). Maleamic acid derivatives can be viewed as a model for carboxypeptidase A, a peptidase with an essential carboxyl group in the active site (*10*). One of the major differences between the hydrolysis of the maleamic acids and the carboxypeptidase A-catalyzed amide hydrolysis is that the optimum pH is about 1 for the former and about 7 for the latter. Besides, the active site zinc ion is essential for carboxypeptidase A-catalyzed reactions.

When the amide nitrogen is a part of a chelating ligand, binding of a Lewis acid to the leaving nitrogen (Eq. [2]) could be facilitated. A maleamic acid derivative containing such an amide nitrogen can be considered as a bifunctional model for carboxypeptidase A, and a well-designed derivative could manifest a large rate acceleration as well as a rate maximum shift to a neutral pH upon addition of a metal ion. We have investigated a series of maleamic acid derivatives for these purposes; and the results with the simplest members, *N*-(2-imidazolylethyl)maleamic acid (**A**), *N*-(2-pyridylethyl)maleamic acid (**B**), and *N*-(2-pyridylmethyl)maleamic acid (**C**) are reported in this article. In addition to being a metal binding site, the heterocyclic ring can provide a positive charge in the vicinity of the amide bond. The effects of the ionization of the heterocyclic nitrogens on the hydrolysis rates have also been examined.

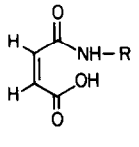

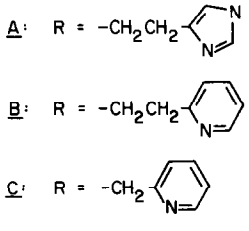

MATERIALS AND METHODS

Materials. Maleamic acid derivatives **A–C** were prepared by adding the solutions of maleic anhydride in chloroform (for **A**) or THF (for **B** and **C**) dropwise to the well-stirred solutions of histamine in chloroform (for **A**), 2-aminoethylpyridine in THF (for **B**), or 2-aminomethylpyridine in THF (for **C**) at 4°C over the period of 30 min. The products were separated as white crystals. Compound **A** was obtained as the histamine salt (mp 129–132°C, sealed tube) which was used without recrystallization due to its hygroscopic nature. Compounds **B** and **C** were recrystallized from THF; mp 131–133°C for **B** and 114–117°C for **C**. Elemental analysis (C,H,N) on **A–C** gave satisfactory results.

Histamine was obtained by neutralizing histamine dihydrochloride (from Aldrich) with sodium hydroxide in methanol, and commercial 2-aminoethylpyridine and 2-aminomethylpyridine (both from Aldrich) were used after distillation. Zinc chloride was obtained from Alfa ("ultrapure") and the solutions of divalent

manganese and cobalt salts were prepared by dissolving manganese (John-Matthey, "specpure") and cobalt (K & K, 99.9%) with hydrochloric acid (Alfa, "ultrapure"). Water was redistilled and deionized before using in the kinetic studies.

Kinetic measurements. Reaction rates were measured with a thermojacketed Beckman Model 25 spectrophotometer. Temperature was controlled to within ±0.1°C with a Haake E 52 circulator. pH measurements were performed with a Chemtrix Type 60 A pH meter. The reactions were carried out at 65°C unless noted otherwise. Evaporation of water during incubation for the kinetic measurements at high temperatures was prevented by sealing the cuvettes tightly with serum caps. Kinetic measurements were usually performed at an ionic strength of 0.05. Over pH 3–4.5 and pH 4.6–5.5, 0.05 *M* formate and 0.05 *M* acetate buffer solutions, respectively, were used. Below pH 3, hydrochloric acid solutions were used. Sodium chloride was added, whenever needed, to maintain the ionic strength at 0.05. For the studies on the metal ion effect, the concentration of the added divalent zinc, manganese, or cobalt chloride was kept at 0.2 *M*. Metal ion itself was used as the buffer species below pH 5 and 0.05 *M* 2-(*N*-morpholino)ethanesulfonate was added above pH 5. The colorimetric determination of 2-aminomethylpyridine was performed with 2,4-dinitrofluorobenzene according to the literature (*11*). The pseudo-first-order rate constants were calculated with the infinity absorbance readings measured or by the Guggenheim method.

RESULTS

Under the conditions of the kinetic measurements, **A** underwent hydrolysis exclusively, as evidenced by the product spectra. The pH dependence of the pseudo-first-order rate constant (k_0) measured at 65°C is illustrated in Fig. 1. The temperature dependence of k_0 measured in 1 *N* hydrochloric acid solutions is illustrated in Fig. 2. The activation thermodynamic parameters derived from the Arrhenius plot are summarized in Table 1.

Incubation of **B** in aqueous buffer solutions produced only the hydrolysis

TABLE 1

THERMODYNAMIC PARAMETERS FOR THE SPONTANEOUS HYDROLYSIS OF A

Parameter[a]	Value
E_a	21.1 ± 2.0 kcal/mol
$\Delta H^{\ddagger}_{39°C}$	20.5 ± 2.0 kcal/mol
$\Delta S^{\ddagger}_{39°C}$	−11.7 ± 7.0 cal/mol · deg
$\Delta G^{\ddagger}_{39°C}$	24.1 ± 0.1 kcal/mol

[a] k_0 at optimum pH at 39°C: $(4.8 \pm 1.1) \times 10^{-3}$ min^{-1} based on the thermodynamic parameters of this table.

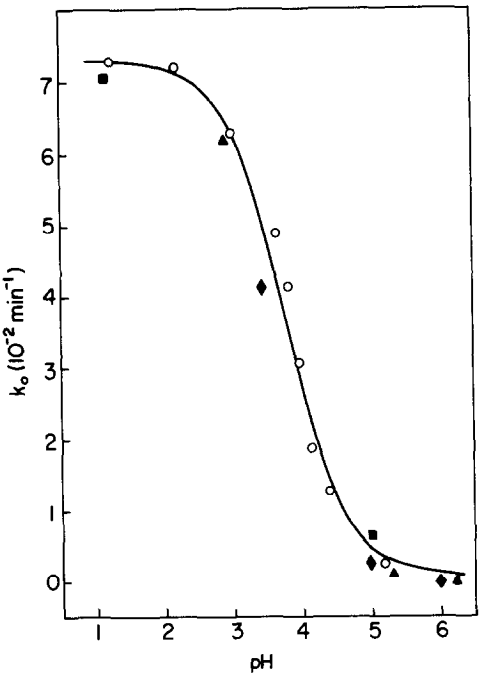

FIG. 1. Kinetic data for the hydrolysis of A. ○, Spontaneous reaction; ■, in the presence of Zn^{2+}; ◆ in the presence of Co^{2+}; ▲, in the presence of Mn^{2+}.

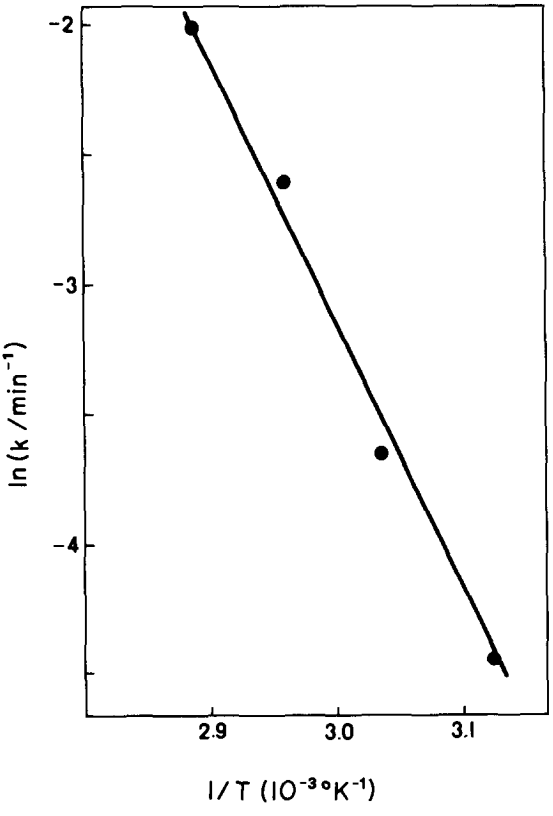

FIG. 2. Arrhenius plot for the hydrolysis of A in 1 *N* hydrochloric acid solutions.

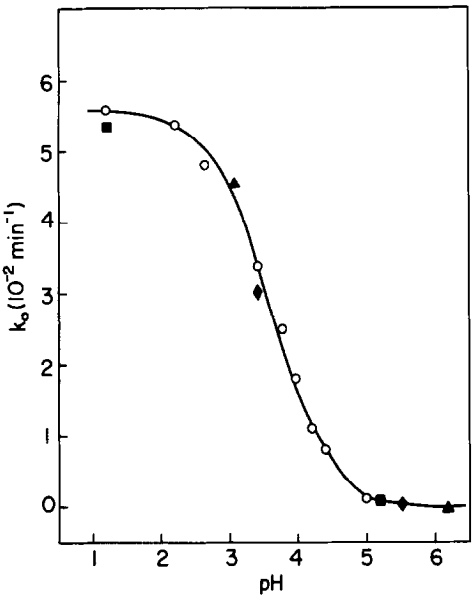

FIG. 3. Kinetic data for the hydrolysis of B. ○, Spontaneous reaction; ■, in the presence of Zn^{2+}; ◆, in the presence of Co^{2+}; ▲, in the presence of Mn^{2+}.

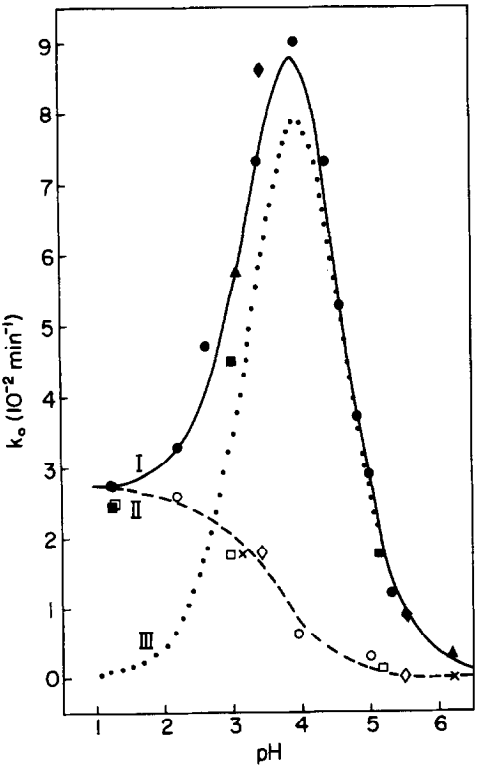

FIG. 4. Kinetic data for the reaction of C. Curve I, total disappearance of C: ●, spontaneous reaction; ■, in the presence of Zn^{2+}; ◆, in the presence of Co^{2+}; ▲, in the presence of Mn^{2+}. Curve II, hydrolytic path: ○, spontaneous reaction; □, in the presence of Zn^{2+}; ◇, in the presence of Co^{2+}; X, in the presence of Mn^{2+}. Curve III, nonhydrolytic path. Curve III is obtained by subtracting curve II from curve I.

products as indicated by the product spectra. The pH dependence of k_0 measured at 65°C is illustrated in Fig. 3.

The absorbance changes of the aqueous solutions of **C** manifested pseudo-first-order kinetics, but the product solutions obtained above pH 2 showed uv spectra which were markedly different from those of the hydrolysis products. When the release of 2-aminomethylpyridine was measured by colorimetric determination with 2,4-dinitrofluorobenzene, the formation of the amine also followed pseudo-first-order kinetics with the same rate constant as that of the absorbance change. On the other hand, the amount of 2-aminomethylpyridine obtained after the completion of the consumption of **C** above pH 2 corresponded to only a fraction of the initially added amount of **C**. Thus, **C** is consumed evidently by parallel reaction paths (Eq. [3]).

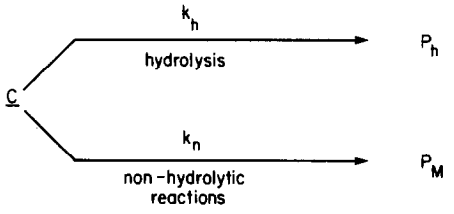

[3]

The pseudo-first-order rate constant for the disappearance of **C** is $(k_h + k_n)$, and this can be calculated from the absorbance changes during the reaction. The amount of 2-aminomethylpyridine obtained after the completion of the reaction relative to the initially added **C** is $k_h/(k_h + k_n)$. Thus, k_h can be calculated from the rate constant for the disappearance of **C** and the amount of 2-aminomethylpyridine released. The corresponding pH dependencies measured at 65°C are illustrated in Fig. 4.

Buffer catalysis was not significant in the hydrolysis of **A–C** when the total concentrations of formate or acetate were varied over 0.01–0.20 *M* at pH 3–5. This indicates the absence of general acid or base catalysis by the buffer species.

The effects of the divalent metal ions on the hydrolysis of **A–C** were examined at various pH's and the results are indicated in the respective pH profiles.

DISCUSSION

pH Effect

The mechanism for the hydrolysis of simple *N*-alkylmaleamic acids is described in Scheme 1 (*3*, *4*). The breakdown of the *N*-protonated tetrahedral intermediate, $T^{\pm}$, leads to the formation of the products. Thus, the unionized form of the maleamic acid is reactive, and the pH profile for this mechanism is a descending sigmoid inflecting at the pK_a of the carboxyl group. The breakdown of $T^{\pm}$ is usually the rate-determining step, and, consequently, the substrate and intermediate in various ionization states are in fast equilibria. The value of k_0 at optimum pH's for the hydrolysis of *N*-methylmaleamic acid at 65°C is 8.9×10^{-2} min^{-1} as

calculated from the kinetic parameters reported in the literature (*3*). This is similar to the corresponding values of **A–C**. Besides, the values of $\Delta H^{\ddagger}$ and $\Delta S^{\ddagger}$ measured with **A** (Table 1) fall within the range of those reported for *N*-alkylmaleamic acids (*3*). Thus, the hydrolysis of **A–C** appears to occur through the same mechanism with the carboxyl group participating as a nucleophile. The absence of general acid or base catalysis by the buffer species indicates that the breakdown of the *N*-protonated tetrahedral intermediate is rate determining for the hydrolysis of **A–C** (*3*, *4*).

The presence of the basic nitrogens in the heterocyclic rings necessitates the inclusion of extra ionization forms in the mechanism for the hydrolysis of **A–C** as summarized in Scheme 2. Some of the kinetically unimportant tetrahedral intermediates are omitted in this scheme. The rate expression derived from this mechanism is

$$k_0 = \frac{k_1K_4[H^+]/K_{a1} + k_2K_5}{[H^+]/K_{a1} + (1 + K_3) + K_{a2}/[H^+]}. \qquad [4]$$

When $k_1K_4 \gg k_2K_5$, the pH profile based on Eq. [4] is a descending sigmoid inflecting at pK_{a1} and the maximum k_0 is k_1K_4. The pH profiles for the hydrolysis of **A–C** are analyzed with Eq. [4], and the parameter values used for the construction of the theoretical curves in Figs. 1, 3, and 4 are summarized in Table 2. The theoretical curves including curve I of Fig. 4 were based on the data points obtained in the absence of the divalent metal ions. The pK_{a1} values obtained for

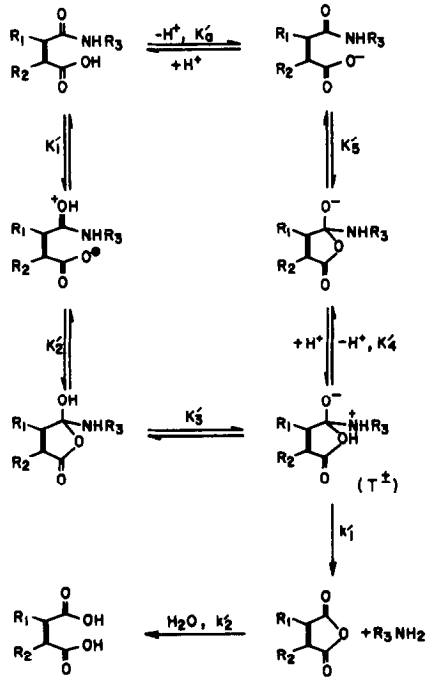

SCHEME 1

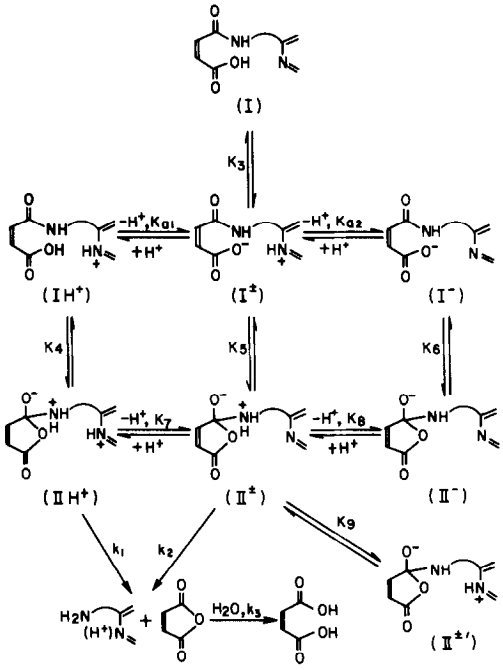

SCHEME 2

A–C agree with those obtained for *N*-alkylmaleamic acids (*3*), and thus can be assigned to the ionization of the carboxyl group.

The descending sigmoids reveal $k_1K_4 \gg k_2K_5$ for the hydrolysis of A–C. Although comparison of K_4 with K_5 is not easily made, it can be done indirectly by comparing K_{a1} with K_7 as K_4K_7 is equal to $K_{a1}K_5$. Ionization of the carboxyl group and the heterocyclic nitrogen is involved in K_{a1} and K_7, respectively. For **A**, the much greater basicity of the imidazole group (pK_a = ca. 7) compared with the carboxyl group (pK_a = 3–4) can lead to $K_4 \gg K_5$ and $k_1K_4 \gg k_2K_5$. For **B** and **C**, comparison of K_{a1} with K_7 is not simple, since the pyridine is not much more basic than the carboxylate and electrostatic effects can be important in the present comparison of the basicities. As will be discussed in the later part of this section, K_{a1} is only about six times greater than K_{a2}. Both K_{a2} and K_7 involve deprotonation of the pyridinium moiety; but the former is accompanied by sacrifice of the favorable electrostatic interaction between the two adjacent opposite charges, while the latter includes relief of the unfavorable electrostatic interaction between the two nearby positive charges. Thus, K_7 is expected to be greater than K_{a2}, and the ratio of K_{a1}/K_7 ($= K_4/K_5$) should be smaller than 6. The descending sigmoids observed for **B** and **C** ($k_1K_4 \gg k_2K_5$) indicates, therefore, that the electrostatic interactions are not significant and/or the breakdown of structure $\mathbf{IIH^+}$ (k_1) is much easier than that of structure $\mathbf{II^\pm}$ (k_2). Thus, the shape of the pH profiles is not affected by the ionization of the heterocyclic nitrogens.

TABLE 2

PARAMETER VALUES USED FOR THE CONSTRUCTION OF THE THEORETICAL pH PROFILES

	k_1K_4 (min^{-1})	pK_{a1}	pK_{a2}	K_s	k_M (min^{-1})
A	7.3×10^{-2}	3.80	—	—	—
B	5.6×10^{-2}	3.60	—	—	—
C	2.7×10^{-2}	3.55	4.35	0.16	1.0

Metal Ion Effect

The rates for the hydrolysis of A–C are not enhanced by the presence of the divalent metal ions, as illustrated in Figs. 1, 3, and 4. Examination of the metal ion effects was extended to higher pH's, where the spontaneous reactions are very slow. This was done because the metal binding could be facilitated when the heterocyclic nitrogens are in the basic forms. Due to the limited solubilities of the metal ions, the study was not extended above pH 6.5.

The absence of metal ion catalysis can be ascribed to the weak binding of the substrate and intermediates to the metal ion. Chelate formation between the substrate and the metal ion can be inefficient due to the weak binding ability of the amide nitrogen. At higher pH's, the tetrahedral intermediate can coordinate to the metal ion (see structure IIM), facilitating the breakdown of the intermediate.

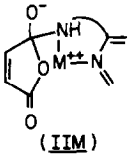

(IIM)

Failure to observe rate acceleration at higher pH's might be a result of inefficient complex formation due to the short lifetime of the intermediate or weak binding. The study has been extended to the derivatives containing tri- and tetradentate ligands, and the results will be the subject of future communication.

Dual Intramolecular Reaction of N-(2-Pyridylmethyl)maleamic Acid

As illustrated in Fig. 4, the pH dependence (curve I) of the disappearance of C has the shape of an unsymmetrical bell. The pH profiles of Fig. 4 indicate the presence of at least three ionization states, each with different reactivities. The results obtained with C were, therefore, further analyzed with Scheme 3.

Structures IH^+–I^- and the constants, except k_M, in this scheme are the same as those in Scheme 2. The products of the hydrolytic and nonhydrolytic paths are denoted by P_h and P_M, respectively. Structures $I^\pm$ and I are in the same ionization state, and the pH profile alone does not reveal which one is responsible for the

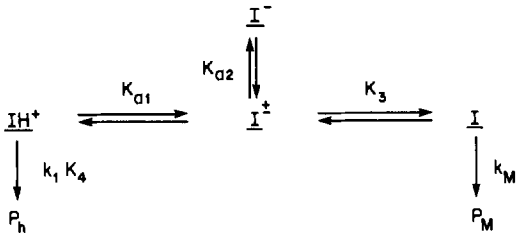

SCHEME 3

formation of P_M. The parameter values obtained from the analysis of curves I[1] and II of Fig. 4 are summarized in Table 2. The pK_{a2} value of 4.35 obtained can be assigned to the ionization of the pyridine moiety, since the spectral titration of C at 65°C (not shown) revealed the pK_a of 4.4 for the pyridine. Curve III of Fig. 4 illustrates the pH profile of the rate constant for the nonhydrolytic path and the general shape of the pH dependencies of the molar fractions of structures $I^{\pm}$ and I.

The nonhydrolytic reaction appears to be the conjugate addition of the pyridine moiety (Eq. [5]).

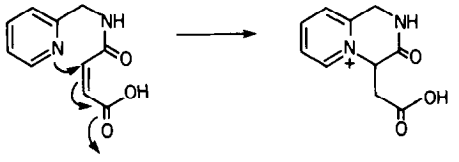

[5]

The absorbances at 270–300 nm of the product solution obtained after incubation at higher pH's were much larger than those of C or the hydrolysis products, in agreement with the formation of the pyridinium salt. The conjugate addition in B would produce a seven-membered lactam, and the failure of the same reaction for B can be ascribed to the transition state of an unfavorable ring size. Lyophilization of a solution of P_M at a neutral pH resulted in the decomposition of the product, while that under acidic conditions retained its integrity, as indicated by the uv spectra. This can be explained by the decarboxylation of the lactam (Eq. [6]). The structure of the reactant in Eq. [5] agrees with the pH profile for the formation of P_M and structure I can be assigned as the reactive form for this reaction.

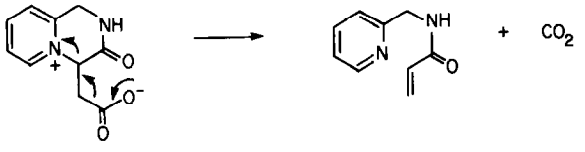

[6]

[1] The rate expression of Scheme 3 which was used for the analysis of curve I is

$$k_0 = (k_1K_4[H^+]/K_{a1} + k_MK_3)/([H^+]/K_{a1} + 1 + K_3 + K_{a2}/[H^+]).$$

The maleamic acid derivative C, therefore, undergoes a dual intramolecular nucleophilic reaction; nucleophilic attack by the carboxyl oxygen at the amide carbon leading to a five-membered ring, and nucleophilic attack by the pyridine nitrogen at the olefinic carbon producing a six-membered ring.

ACKNOWLEDGMENT

Support of this investigation by a grant from the Korea Science and Engineering Foundation is gratefully acknowledged.

REFERENCES

1. A. J. KIRBY AND A. R. FERSHT, "Progress in Bioorganic Chemistry" (E. T. Kaiser and F. J. Kézdy, Eds.), Vol. 1, pp. 1–82. Wiley, New York, 1971.
2. D. P. N. SATCHELL AND R. S. SATCHELL, "Annual Reports on the Progress of Chemistry," Vol. 75, Sect. A, pp. 25–48. The Chemical Society, London, 1979.
3. A. J. KIRBY AND P. W. LANCASTER, *J. Chem. Soc. Perkin Trans. 2,* 1206 (1972).
4. M. F. ALDERSLEY, A. J. KIRBY, P. W. LANCASTER, R. S. MCDONALD, AND C. R. SMITH, *J. Chem. Soc. Perkin Trans. 2,* 1487 (1974).
5. A. J. KIRBY, R. S. MCDONALD, AND C. R. CLINTON, *J. Chem. Soc. Perkin Trans. 2,* 1495 (1974).
6. R. KLUGER AND C.-H. LAM, *J. Amer. Chem. Soc.* **97,** 5536 (1975).
7. R. KLUGER AND C.-H. LAM, *J. Amer. Chem. Soc.* **100,** 2191 (1978).
8. R. KLUGER, J. CHIN, AND W.-W. CHOY, *J. Amer. Chem. Soc.* **101,** 6976 (1979).
9. R. BRESLOW AND D. E. MCCLURE, *J. Amer. Chem. Soc.* **98,** 258 (1976).
10. J. SUH AND E. T. KAISER, *J. Amer. Chem. Soc.* **98,** 1940 (1976).
11. M. PESEZ AND J. BARTOS, "Colorimetric and Fluorimetric Analysis of Organic Compounds and Drugs," pp. 129–130. Dekker, New York, 1974.